

Geophysical Research Letters

RESEARCH LETTER

10.1029/2019GL086561

Key Points:

- We present the first year round record of calving activity at a lacustrine ice-margin and classify 216 calving events by mechanism and volume
- Melt-undercutting and the presence and absence of lake ice cover are associated with seasonality in calving rates and processes
- Lengthening summer seasons and thinning ice-margins are likely to increase calving rates and thus rates of mass loss at lacustrine margins

Supporting Information:

- Supporting Information S1

Correspondence to:

J. Mallalieu,
j.mallalieu@leeds.ac.uk

Citation:

Mallalieu, J., Carrivick, J. L., Quincey, D. J., & Smith, M. W. (2020). Calving seasonality associated with melt-undercutting and lake ice cover. *Geophysical Research Letters*, *47*, e2019GL086561. <https://doi.org/10.1029/2019GL086561>

Received 10 DEC 2019

Accepted 30 MAR 2020

Accepted article online 9 APR 2020

© 2020. The Authors.

This is an open access article under the terms of the Creative Commons Attribution License, which permits use, distribution and reproduction in any medium, provided the original work is properly cited.

Calving Seasonality Associated With Melt-Undercutting and Lake Ice Cover

Joseph Mallalieu¹ , Jonathan L. Carrivick¹ , Duncan J. Quincey¹, and Mark W. Smith¹

¹School of Geography and Water@Leeds, University of Leeds, Leeds, West Yorkshire, UK

Abstract A detailed understanding of calving processes at the lacustrine margins of the Greenland ice sheet is necessary for accurately forecasting its dynamic response to ongoing climate change. However, existing data sets of lacustrine calving are limited to summer seasons and to alpine glaciers. Here, we use an integrated time-lapse and structure-from-motion approach to generate the first continuous year-round volumetric record of calving processes at a lacustrine ice sheet margin. We identify two distinct calving regimes that are associated with melt-undercutting and lake ice cover. We also find that calving rates respond rapidly to sudden lake drainage. Given that lake temperature, lake ice cover, and sudden lake drainages are controlled by air temperature and ice-margin thinning, we suggest that climate change, manifested in lengthening summer seasons, will accelerate rates of mass loss and terminus recession at lacustrine ice-margins in Greenland.

Plain Language Summary Lakes situated at the margins of glaciers and ice sheets are important because they promote the detachment of large blocks of ice to form icebergs, a process known as calving. Climate change is increasing the number of lakes at the margins of the Greenland ice sheet, and many of those already present are increasing in size. Consequently, a detailed understanding of lake calving processes is needed to accurately predict the future response of the ice sheet to climate change. This study improves our knowledge of calving processes by using time-lapse cameras to record images of calving activity at a lake located in western Greenland over a continuous 14-month period. We use the images to create 3D models that illustrate how calving processes change through time and find that rates and styles of calving vary seasonally in response to lake-driven undercutting of the ice sheet margin and the presence or absence of lake ice cover. Our results suggest that ice loss via calving activity at the lake edges of the Greenland ice sheet will increase in future as summer seasons lengthen in response to climate change.

1. Introduction

The Greenland ice sheet (GrIS) has lost mass at an accelerated rate since the late 1990s and is one of the largest individual contributors to current and predicted sea-level rise (Gillet-Chaulet et al., 2012; Hanna et al., 2013; Jiang et al., 2010; Kjeldsen et al., 2015; Van Den Broeke et al., 2016; Velicogna, 2009). Approximately half of the mass lost from the GrIS occurs at water-terminating margins and can be attributed to a combination of calving and subaqueous melt, which together comprise frontal ablation (Khan et al., 2015; Van Den Broeke et al., 2009). Existing efforts to quantify calving dynamics in Greenland have focused on several large, marine-terminating outlet glaciers responsible for draining the ice sheet interior (e.g. Medrzycka et al., 2016; Murray et al., 2015; Rignot et al., 2015; Ryan et al., 2015). However, the lacustrine calving margins of the GrIS have received comparatively little attention despite (i) ~12% of the western margin of the GrIS terminating in a lake, (ii) a substantial increase in the number and area of ice-marginal lakes over the last three decades, and (iii) an expectation that they will continue to expand into the future (Carrivick & Quincey, 2014; Carrivick & Tweed, 2019). Specifically, the growth of ice-marginal lakes at the GrIS margin is significant in the short term because of their propensity to accelerate rates of mass loss and ice-margin recession through a range of thermo-mechanical controls, including the onset and promotion of calving (Carrivick & Tweed, 2013). These effects on glacier dynamics have been extensively documented in alpine environments (e.g., Boyce et al., 2007; King et al., 2018; Kirkbride, 1993; Trussel et al., 2013; Tsutaki et al., 2011). On longer timescales, the relative importance of lacustrine controls on ice-margin dynamics in Greenland will increase as marine termini recede onto land (e.g., Joughin et al., 2010; Nick et al., 2013), while the growth and coalescence of ice-marginal lakes has also been identified as a key factor controlling ice stream initiation and rapid ice sheet collapse (Demidov et al., 2006; Perkins &

Brennand, 2015; Stokes & Clark, 2003; Stokes & Clark, 2004). Consequently, a detailed understanding of the lacustrine margins of the GrIS is necessary to accurately forecast its dynamic response to ongoing climate change.

Lacustrine calving rates are typically an order of magnitude lower than those from marine environments (Benn et al., 2007; Truffer & Motyka, 2016). However, a sparsity of quantitative data means that calving processes and their associated drivers at lacustrine ice-margins remain poorly understood (Purdie et al., 2016; Trussel et al., 2013). Consequently, the relative importance of lacustrine calving to ice-margin dynamics remains challenging to assess. The scarcity of lacustrine calving data sets stems partially from the methodological challenges associated with acquiring long-term quantitative records of calving in highly dynamic and hazardous environments (Mallalieu et al., 2017; Purdie et al., 2016). In particular, the climatic and financial constraints of fieldwork in glacial regions restrict most calving studies to the melt season, thus neglecting important seasonal variations in calving rates and processes. Where extended records of calving do exist, for example, via the use of time-lapse photography, they typically lack the volumetric data necessary to link calving event magnitude to mechanisms and drivers of change (e.g., Amundson et al., 2010). Recently, integration of time-lapse photography with structure-from-motion (SfM) techniques (e.g., Eltner et al., 2016; Mallalieu et al., 2017) has facilitated the long-term investigation of geomorphological change through the acquisition and analysis of multitemporal topographic point clouds at fine spatiotemporal resolutions. These methods offer great potential for the characterization and quantification of the complex calving processes driving mass loss at water-terminating ice-margins over extended durations.

In this study, we adopt an integrated time-lapse and SfM approach to quantify calving processes at a lacustrine margin of the GrIS using multitemporal point clouds. Specifically, we aim to (i) present the first extended (>1 year) volumetric record of calving from a lacustrine ice-margin, (ii) analyze spatial and temporal patterns in calving event frequency, volume, and mechanism throughout the survey duration, and (iii) opportunistically explore the effects of two discrete lake drainage events on calving processes and ice-margin stability.

2. Data and Methodology

2.1. Study Site

We present a record of calving from a $\sim 1\text{-km}^2$ ice-dammed lake ($67^{\circ}08'10''$ N, $50^{\circ}04'25''$ W) situated on the northern margin of Russell Glacier, a terrestrial outlet of the GrIS in western Greenland (Figure 1). The lake, hereafter referred to as Russell Glacier ice-dammed lake (IDL), is notable for annual sudden and extremely rapid drainage events via a subglacial conduit situated in its southwestern corner (Russell et al., 2011). Following gauging of lake drainage events in 2010 and 2012, Carrivick et al. (2017) invoked localized flotation of the ice dam as the mechanism initiating lake drainage, based on (i) water depths exceeding 40 m and a maximum ice dam thickness in the southwestern corner of the lake of ~ 50 m and (ii) a numerical model demonstrating that the extremely rapid water egress could not be fully explained by thermo-erosion and conduit melt-widening. Ice-surface velocities in the vicinity of Russell Glacier IDL are $\sim 30\text{ m a}^{-1}$ (Rignot & Mouginot, 2012).

2.2. Image Acquisition and Point Cloud Generation

Point clouds of ice-margin geometry were generated using an integrated time-lapse and SfM approach described and evaluated in detail in Mallalieu et al. (2017). Consequently, a reduced synopsis is provided here. The primary data set comprised an image archive of ice-margin dynamics spanning 426 days between 27 July 2014 and 20 September 2015, acquired via the installation of an array of fifteen trail cameras around the lake shore (Figure 1). The extensive image overlap afforded by the cameras was exploited using SfM processing in Agisoft PhotoScan Professional (v. 1.4.2) to construct dense point clouds of ice-margin geometry from discrete image sets. Point clouds were georeferenced and scaled using a network of 18 ground control points established on stable landscape features adjacent to the ice-margin, and subsequently cropped to the area of greatest camera overlap to maintain high point densities. The resulting point clouds consistently captured the geometry of a $\sim 550\text{-m}$ wide stretch of the calving margin, accounting for $\sim 60\%$ of the total lake-ice interface.

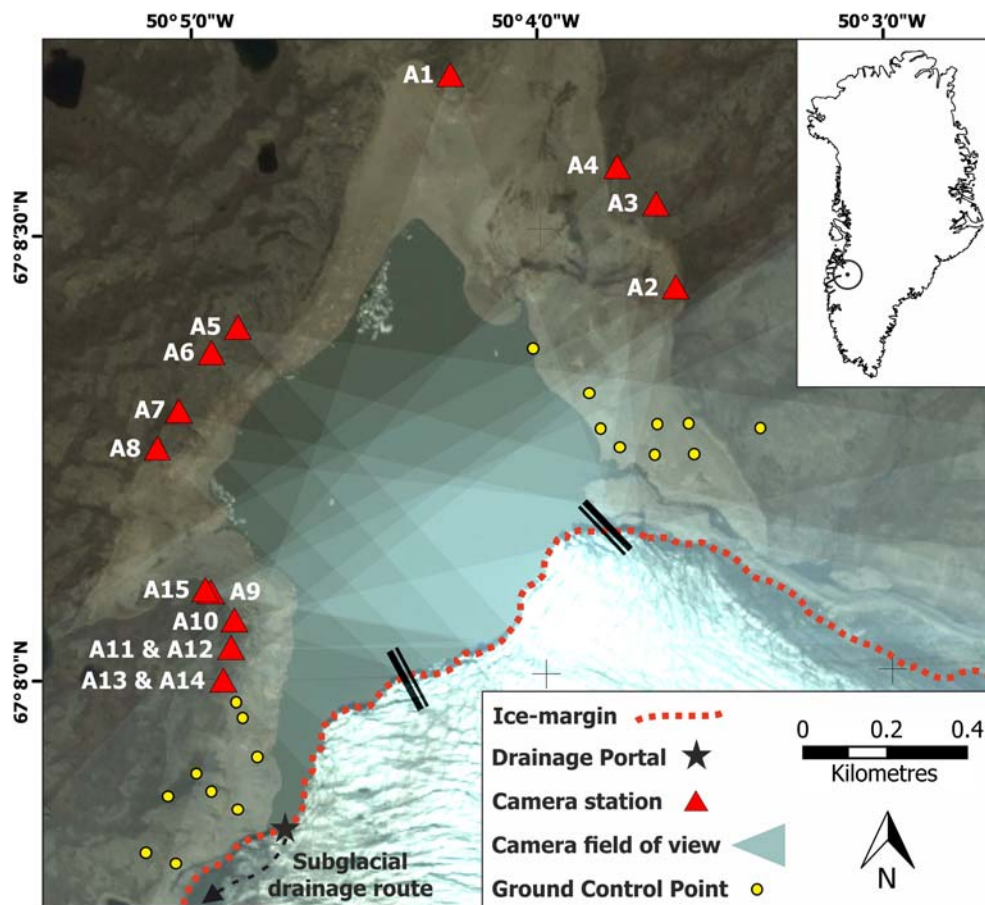


Figure 1. Camera array setup and study location on the northern margin of Russell Glacier, western Greenland (inset). Heavier blue shading represents increased camera overlap. Black bars delineate the extent of the cropped ice-margin point clouds employed in the analysis, adapted from Mallalieu et al. (2017).

2.3. Point Cloud Analysis

In order to perform a seasonal analysis of calving processes, point clouds were generated at $7 (\pm 1)$ day intervals throughout the bulk of the survey period, with sampling frequency reduced to $28 (\pm 2)$ day intervals between November 2014 and April 2015 to reflect decreased activity at the ice-margin (Table S1 in the supporting information). The minor variations in sampling interval were caused by inclement weather conditions preventing the acquisition of viable imagery for SfM processing. In addition to the seasonal calving analysis, extra point clouds were generated with enhanced frequency around lake drainage events on 3 August 2014 and 28 July 2015 to investigate their effect on calving processes (Table S1). A volumetric record of calving losses throughout the survey duration was established via the differencing and analysis of 56 successive point clouds using CloudCompare (v. 2.9.1). Details of the point cloud processing and analysis are provided in Text S1, Figure S1, and Tables S2 and S3).

2.4. Calving Classification

Recent advances in discrete element modeling have identified three broad mechanisms associated with calving: ice-cliff failure, undercut calving, and buoyancy-driven calving (Åström et al., 2013; Benn et al., 2017). However, associated calving criteria remain untested due to a lack of quantitative observational records. In this study, a classification system for determining the mechanism of individual calving events was developed by assessing the nature of resultant geometric changes at the ice-margin and refining existing calving categorizations, principally those of Minowa et al. (2018) and How et al. (2019). Particular attention was paid to whether events (i) occurred at or above the waterline, (ii) extended the full height of the ice-cliff, and (iii) demonstrated outward rotation from the ice-cliff prior to failure. Events were subsequently categorized into five classes: ice-falls, topples, impact events, waterline events, and collapses (Figure 2). The characteristics of

key mechanisms are presented in Figure S2 using multitemporal 2D profiles of the ice-cliff. No evidence of subaqueous calving was observed over the duration of the study. Details of the meteorological and lake data sets used to investigate environmental controls on calving processes are provided in Text S2.

3. Results

3.1. Calving Event Attributes

Over the course of our study period, 216 calving events were detected, amounting to total calving losses of 1.05 M m^3 (Table S4). Individual calving events ranged from 4 to $12,719 \text{ m}^2$ in area, with a mean of 808 m^2 ; while event volumes ranged from 3 to $80,148 \text{ m}^3$, with a mean of $4,888 \text{ m}^3$. The volume-area ratio of calving events was approximately 1:1 for small magnitude events but rose to 10:1 for the largest events, suggesting that large magnitude events possessed a proportionally greater depth than their smaller counterparts (Figure S3). Magnitude-frequency analysis of event volume indicated that total calving losses over the survey duration were dominated by infrequent, but high magnitude events, with the largest 10 events cumulatively accounting for 52% of total mass lost, whereas the smallest 100 events accounted for <1% of the total volume. Ice-fall was the most frequent calving mechanism, accounting for 38% of all events, followed by waterline events (26%), topples (19%), collapses (13%), and impact events (4%). Calving mechanisms were also typified by disparities in event volume, with collapses possessing the largest mean volume ($23,512 \text{ m}^3$), followed by topples ($7,013 \text{ m}^3$), waterline events ($1,078 \text{ m}^3$), and the notably smaller ice-fall (305 m^3) and impact events (284 m^3) (Table S4, Figure S3). Consequently, collapses and topples were the dominant calving mechanisms over the survey duration, accounting for 63% and 29% respectively of total mass lost, with the remaining 8% of losses attributed to waterline, ice-fall, and impact events (Table S4).

3.2. Seasonal Variability in Calving Dynamics

Temporal analysis of the seasonal data set identified distinct cycles in calving properties (Figure 3). The highest calving rates and monthly calving volumes were typically associated with the months of August and September, while low calving rates characterized the period between December and July (Figures 3d and 3e). Perhaps unexpectedly, calving rates remained relatively high throughout October and November, despite the onset of lake freeze in late September (Figure 3c). Conversely, calving rates remained low throughout July even after the full thawing of the lake in late June. Calving event frequency followed a similar seasonal cycle, with the exception of June 2015 when a high number of ice-falls coincided with the return of positive air temperatures (Figures 3a and 3g). The onset of lake freezing and thawing coincided with notable changes in both the number of calving events and the contribution of each mechanism to the total calving volume (Figures 3c and 3f). In the months of August and September, the collapse mechanism accounted for the vast majority of calving losses, whereas topples became the dominant driver of mass loss from October until the end of June. The only outlier occurred in July when waterline events contributed the majority of mass loss.

The seasonal cycle of ice-margin advance and recession was broadly synchronous with changes in calving rate, whereby ice-margin recession was associated with high calving rates in summer, and advection occurred when calving rates were minimal in winter (Figure 3). For the period in which the lake remained frozen, a significant positive correlation ($p < 0.05$) was identified between air temperature and calving event frequency. While the lake remained unfrozen, significant negative correlations ($p < 0.05$) were identified between calving rate and lake volume, and calving rate and the rate of lake volume change (Figure S4).

3.3. Effects of Sudden Lake Drainage on Calving Dynamics

Two lake drainage events occurred during the survey period. The first, on 3 August 2014, caused a fall in lake stage of 15.60 m over a ~41-hr period, corresponding to a reduction in lake volume of 8.05 M m^3 . The second event occurred on 28 July 2015 with a fall in lake stage of 12.65 m over ~44 hr, corresponding to a reduction of 6.41 M m^3 in lake volume (Figure 4, Table S1). Both events revealed the presence of a ~1.5-m deep thermo-erosional notch spanning the ice-cliff at the maximum elevation of the lake level (Figures 4 and S2a). Calving activity in the six days prior to the 2014 drainage event was dominated by collapse, waterline, and ice-fall events (Figure 4), representative of the operative calving mechanisms during the months of August and September in the seasonal calving survey (Figure 3g). During the drainage event itself, calving activity was dominated by a series of discrete ice-falls immediately above the newly exposed



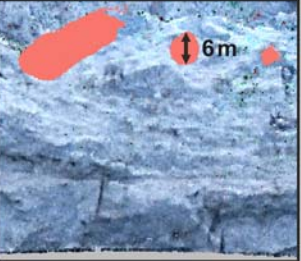


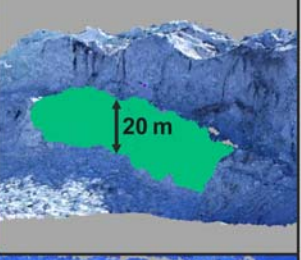





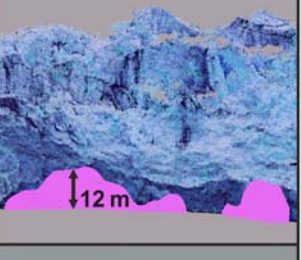


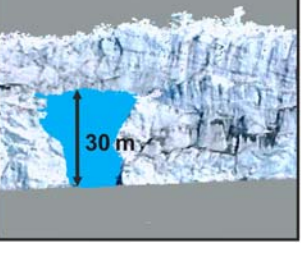
Classification	Pre-calving imagery	Post-calving imagery	Differenced point cloud
<p>Ice-fall: Small-medium size events. Blocks of ice fall from ice-cliff, typically from higher-elevations. Triggered by structural weaknesses within the ice and/or undercutting at the waterline.</p>	 <p>17 Aug 2014</p>	 <p>24 Aug 2014</p>	 <p>6m</p>
<p>Topple: Medium-large events. Outward toppling of sheets and stacks of ice, indicative of outward force imbalance at ice-cliff. Failure does not propagate down to water level.</p>	 <p>7 June 2015</p>	 <p>14 June 2015</p>	 <p>20m</p>
<p>Impact: Small events triggered by impact of falling ice from higher elevations. Typically found on relaxed gradients below vertical or overhanging faces. Associated with Fall and Topple events.</p>	 <p>12 Dec 2014</p>	 <p>Block falls by toppling</p> <p>Site of impact</p> <p>10 Jan 2015</p>	 <p>9m</p>
<p>Waterline: Small-medium events. Blocks of ice detach at the waterline. Typically associated with undercutting by a thermo-erosional notch.</p>	 <p>15 Sept 2014</p>	 <p>21 Sept 2014</p>	 <p>12m</p>
<p>Collapse: Medium-large events. Collapse of sheets and stacks of ice spanning the full height of the ice-cliff. Likely to be facilitated by both undercutting and outward force imbalance.</p>	 <p>1 Aug 2014</p>	 <p>2 Aug 2014</p>	 <p>30m</p>

Figure 2. Classification of the five calving mechanisms observed at Russell Glacier IDL, based on geometric changes at the ice-margin (determined via point cloud differencing), interpretation of camera imagery precalving and postcalving, and existing calving categorizations. Approximate calving event magnitudes are indicated by the scale bars on the differenced point clouds.

thermo-erosional notch (Figures 4 and S2c). In the three days subsequent to the lake drainage, calving losses were dominated by waterline, ice-fall, and topple events, but within six days patterns and mechanisms of calving broadly mirrored those prior to the drainage event. Calving activity during the 2015 lake drainage replicated the patterns observed in 2014 but with the absence of any collapse events prior to and topple events subsequent to the lake drainage. Notably, high-magnitude collapse events were observed within six days of both the 2014 and 2015 lake drainage (Figure 4).

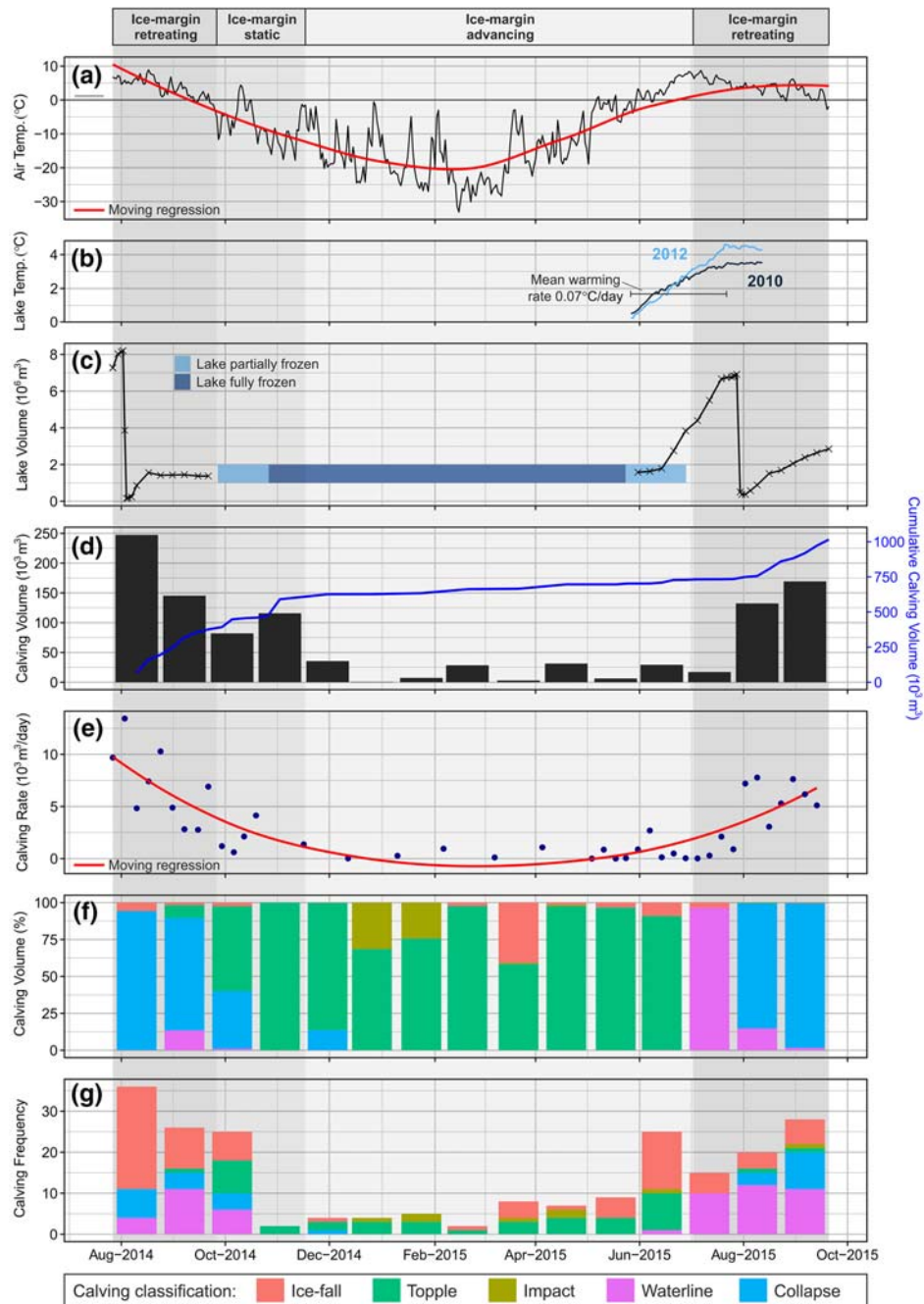


Figure 3. Seasonal record of calving, lake and meteorological activity at Russell Glacier IDL between 27 July 2014 and 20 September 2015. (a) Mean daily air temperature; (b) mean daily lake temperature from spring 2010 and 2012 (from Carrivick et al., 2017); (c) lake volume, indicating onset of lake freeze/thaw and occurrence of drainage events on 3 August 2014 and 28 July 2015; (d) calving volume and cumulative calving volume over the survey duration; (e) calving rate; (f) calving volume by mechanism (%); (g) calving frequency by mechanism. Note that calving data were measured at $7 (\pm 1)$ day intervals from 27 July to 19 Oct 2014 and 11 May to 20 Sept 2015 but are aggregated and plotted here at 28-day intervals to maintain a consistent sampling interval across the survey.

4. Discussion

4.1. Calving Processes

Comparison of calving activity across multiple sites is challenging due to the absence of a standardized system for classifying observed calving events and divergent techniques for measuring event magnitude. However, the magnitude-frequency distribution of calving events observed at Russell Glacier IDL broadly replicates existing records from both lacustrine (e.g., Minowa et al., 2018; Warren et al., 1995) and marine

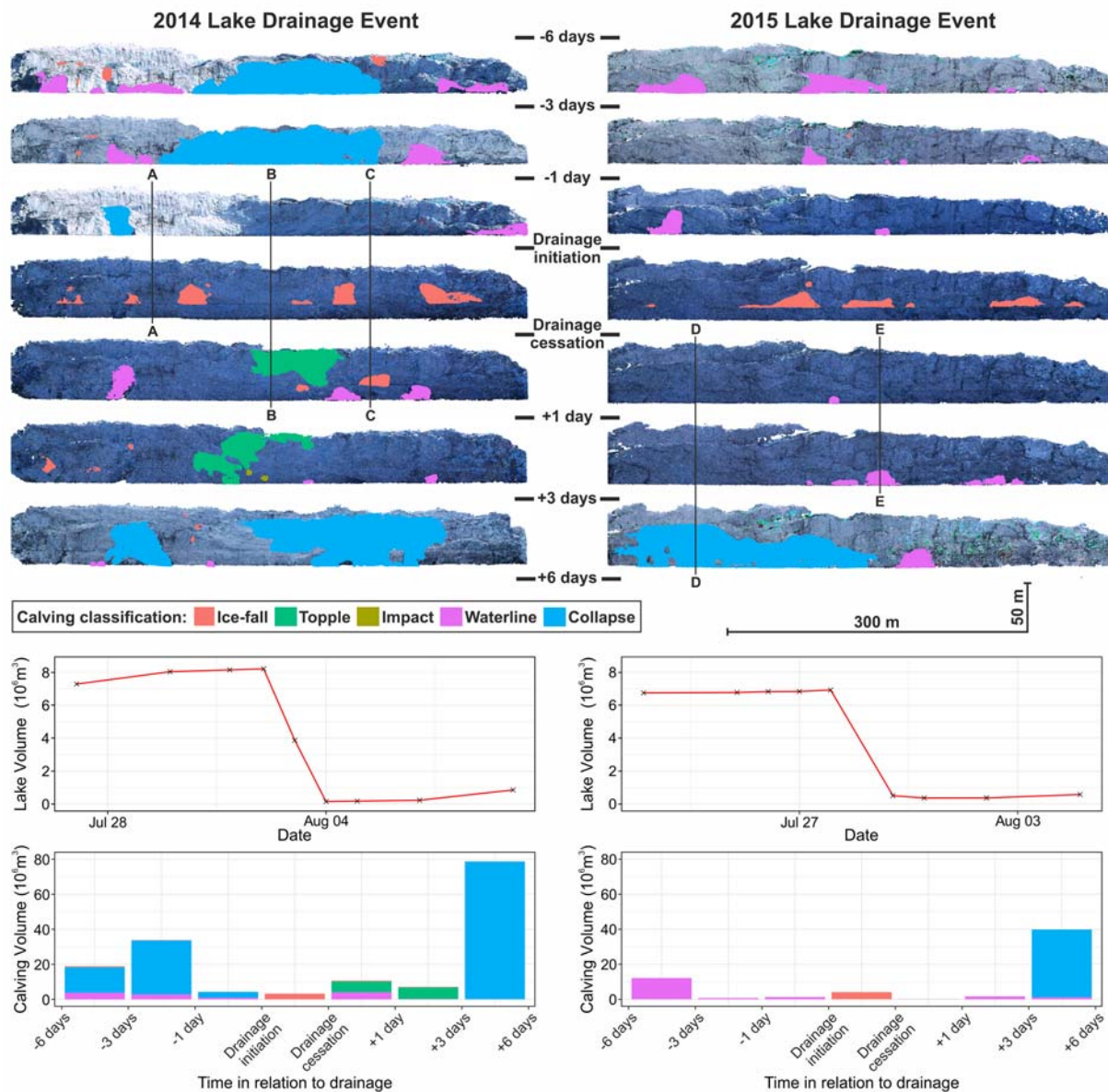


Figure 4. Spatiotemporal record of calving associated with lake drainage events commencing on the 3 August 2014 and 28 July 2015. Transects A–E denote the positions of the 2D ice-cliff profiles illustrated in Figure S2.

termini (e.g., Chapuis & Tetzlaff, 2014; How et al., 2019; Medrzycka et al., 2016), whereby relatively low-magnitude falls are the most prevalent calving mechanism, but mass loss is dominated by a small number of high-magnitude events.

The propagation of undercuts via subaqueous melting below the waterline is integral to calving processes because they increase force imbalances at the terminus and promote calving failures (Benn et al., 2007). Recent efforts by Benn et al. (2017) to simulate these calving processes at marine termini via discrete element modeling showed that undercutting of the calving front is associated with two magnitudes of calving event. Low-magnitude events occurred where the loss of support by undercutting exacerbated existing faults in the ice-cliff, causing localized, shallow subaerial failures, whereas high-magnitude events were associated with the propagation of suitably orientated surface fractures and outward bending of the ice-cliff over the undercut, leading to the collapse of the entire ice column. Our observations and volumetric measurements of ice-fall and collapse events at Russell Glacier IDL (Figure 2, Table S4) therefore provide compelling

evidence for these modeled low- and high-magnitude calving mechanisms respectively and suggest that these processes are similar at both marine and lacustrine termini.

The extensive occurrence of waterline and collapse events across the width of the calving front at Russell Glacier IDL (e.g., Figure 4) suggests that melt-undercutting via thermo-erosional notch propagation is the primary control on calving losses and that, when the lake is ice-free, the long-term calving rate will therefore be related to the rate of undercutting. In addition, the presence of a thermo-erosional notch, rather than undercut, at the waterline (Figures S2a and S2c) illustrates an element of stratification in lake temperature. Such stratification in water temperature could conceivably also exist at tidewater glacier margins. Few measurements of notch propagation at lacustrine margins exist due to their inherently hazardous nature, but rates of 0.8 m day^{-1} have been reported from Glaciar Leon (Haresign & Warren, 2005) and 0.2 to 0.3 m day^{-1} from both the Miage (Diolaiuti et al., 2006) and Tasman (Röhl, 2006) glaciers. Although we lack direct measurements here, such rates would not be inconceivable at Russell Glacier IDL because extensive waterline failures (exceeding the 0.5-m depth detection threshold) were observed within 24 hr of the 2014 lake drainage and 72 hr of the 2015 lake drainage, both of which significantly lowered lake level and thus reset notch formation (Figure 4). Because lake drainage at Russell Glacier IDL is flotation triggered, a transition from undercut driven calving to buoyancy driven calving, as documented at other lacustrine termini following downwasting (e.g., Boyce et al., 2007; Dykes et al., 2011; Trussel et al., 2013), remains unlikely despite recent observations of surface thinning (Carrivick et al., 2017).

4.2. Seasonal Variability in Calving Dynamics

Calving activity at Russell Glacier IDL can be characterized into two distinct temporal regimes that are broadly coincident with the presence and absence of lake ice cover. While the lake remains ice-free, calving processes and mass loss are driven by melt-undercutting, whereas following lake freeze calving is driven by force imbalances at the terminus that promote the outward toppling of unstable flakes and pillars of ice (Figures 3c and 3f). The significant reduction in calving rates and monthly calving volumes commencing in December 2014 is hypothesized to be a consequence of calved material accumulating on the frozen lake surface throughout the autumn increasing buttressing of the calving front and thus suppressing further events (see topple image in Figure 2). The low calving rates observed in July 2015 are indicative of limited melt-undercutting despite the break-up of lake ice in the preceding month. However, records of lake temperature from 2010 and 2012 indicate that this time period coincided not only with the warming regime of the lake but also with rapid increases in lake level (Figures 3b and 3c). Such high rates of lake level rise are likely to have significantly inhibited rates of melt-undercutting due to the dissipation of thermal energy over a greater elevation range (cf. Röhl, 2006). Suppression of calving rates by lake level fluctuations is also evidenced by the significant negative correlation identified between calving rate and the rate of lake volume change (Figure S4a). The $\sim 10\text{-m}$ rise in lake level between mid-June and late July 2015 is hypothesized to have inhibited calving processes associated with outward force imbalances over this period by reducing stress gradients at the calving front. In addition, the presence of a significant negative correlation between lake volume and calving rate (Figure S4a) also indicates that elevated lake levels restricted the magnitude of calving events by diminishing the vertical extent of the subaerial calving front.

Together these findings suggest that thermo-erosional notch development and associated ice-cliff collapse is the primary physical explanation for the recorded seasonal variability in calving activity. The observed ice-margin advance throughout winter and spring could arise from the process no longer operating, whereas ice-margin recession in summer is most likely driven by the resumption of melt-undercutting following lake warming (Figure 3). Furthermore, the seasonal advance and recession of the ice-margin coincides with the formation and disintegration of lake ice cover. In this regard, the dynamics of lacustrine termini appear similar to the observed relationships between tidewater glaciers and ice-melange, whereby tidewater termini advance and retreat in response to the presence or absence of buttressing by an ice-melange, respectively (Amundson et al., 2010; Cassotto et al., 2015; Vieli et al., 2002; Xie et al., 2019).

This study demonstrates that both lake thermal regime and lake ice cover could act as substantial controls on calving processes at lacustrine termini. Therefore, climate-driven changes to lake water temperatures and ice cover regimes may have significant potential for perturbing rates of mass loss at calving margins and consequently lacustrine ice-margin dynamics. For example, studies of non-ice-contact lakes in the Arctic region have identified a progressive earlier break-up of winter ice cover and extension of ice-free days in

response to atmospheric warming in recent decades (Duguay et al., 2006; Smejkalova et al., 2016; Surdu et al., 2016). At lacustrine margins, similar shifts in ice cover regime would extend the duration of the calving season associated with higher magnitude calving events (e.g., melt-undercut-induced collapses), accelerating rates of mass loss, and potentially initiating a positive feedback whereby enhanced ice-margin recession, lake expansion, and glacier thinning create favorable conditions for a transition from melt-undercutting to buoyancy-driven calving, which has been associated with the rapid disintegration of several lacustrine termini in alpine environments (e.g., Boyce et al., 2007; Tsutaki et al., 2013). Similar responses have been observed at several Greenlandic tidewater outlets where terminus recession has been linked to reductions in sea ice duration and the earlier onset of melange disintegration (e.g., Christoffersen et al., 2011; Howat et al., 2010; Joughin et al., 2008). However, we note that the sensitivity of ice-marginal lakes in Greenland to atmospheric warming is unlikely to be uniform, because (i) the ice cover regime of Arctic lakes is primarily controlled by lake geometry (Arp et al., 2010) and (ii) the presence or absence of glacial meltwater inputs further complicates the seasonal evolution of proglacial lake thermal regimes (Carrivick & Tweed, 2013).

4.3. Effects of Sudden Lake Drainage on Calving Dynamics

Although immediate calving responses to the 2015 lake drainage were confined to discrete ice-falls along the thermo-erosional notch, the subsequent topple events under ice-free lake conditions are indicative of increased stress gradients at the calving front promoting the outward toppling of unstable flakes and pillars of ice in response to debuttressing. Similarly, How et al. (2019) observed that calving termini are highly sensitive to variations in backstress, with even relatively small reductions, such as those associated with the falling limb of an ocean tide, observed to increase calving frequency. The recurrence of waterline events within 24 hr of both the 2014 and 2015 lake drainages implies rapid reestablishment of melt-undercutting as the dominant driver of calving at Russell Glacier IDL. However, increased stress gradients promoting the outward bending of the ice-cliff over a newly formed undercut may also account for the large collapse events recorded within 6 days of both the 2014 and 2015 lake drainages and thus signify the additional presence of a delayed process response to lake drainage. Consequently, the capacity of lake drainage events to perturb dominant calving processes appears temporally limited, although, provided that the lake does not fully drain, calving rates are likely to increase in the aftermath of lake drainages due to the increased vertical extent of the subaerial calving front. There has been no analysis of the impact of sudden lake drainages on ice-margin dynamics regionally, despite recognition of the increasing number of both ice-marginal lakes (Carrivick & Quincey, 2014) and sudden ice-marginal lake drainages (Carrivick & Tweed, 2019) around the GrIS.

5. Conclusions

This study has presented the first extended (>1 year) volumetric record of calving losses at a lacustrine ice-margin. The associated data set has enabled recognition of two distinct calving regimes: when the lake is ice-free, high calving rates are driven by processes associated with thermally driven melt-undercutting, whereas when the lake is frozen lower calving rates are driven by force imbalances at the ice-cliff. We also infer that a further reduction in calving activity in the winter months is a response to the buttressing effect of previously calved material accumulating in front of the ice-margin on the frozen lake surface. Consequently, changes to lake water temperature and to seasonal lake ice cover, as would be expected with warmer and lengthening summers with climate change, could have significant implications for rates of mass loss and thus wider lacustrine ice-margin dynamics. In addition, sudden lake drainage events were observed to have a temporally limited impact on calving activity, with dominant calving processes reestablishing within days of lake drainage. However, calving rates did increase following lake drainage events due to the increased vertical extent of the subaerial calving front. More widely, the integration of time-lapse photography and SfM techniques is well suited to the acquisition of volumetric calving records from glacier termini and, with advances in the automation of point cloud workflows and the remote-transmission of imagery, has considerable potential to facilitate the real time acquisition of volumetric calving records and investigation of calving processes at the event scale.

Acknowledgments

Funding to support the acquisition, installation, and maintenance of the camera array was provided by the Royal Institute of Chartered Surveyors Research Trust (project number 474); the Mount Everest Foundation; the Gilchrist Educational Trust; Sigma Xi; and the River Basin Processes and Management research cluster in the School of Geography at the University of Leeds. JM is funded by a Graduate Assistantship from the School of Geography at the University of Leeds. The authors would like to thank Will James for assistance in the field, Alun Hubbard for providing meteorological data from Point 660, and Cassandra Raby for support presenting the figures. The authors would also like to thank Poul Christoffersen and an anonymous reviewer for their valuable comments and insights, which helped improve this manuscript. The data presented here are available via the UK Polar Data Centre: <https://doi.org/10.5285/5CC71534-7F97-4974-8271-D407F1188E2F>.

References

- Amundson, J. M., Fahnestock, M., Truffer, M., Brown, J., Lüthi, M. P., & Motyka, R. J. (2010). Ice mélange dynamics and implications for terminus stability, Jakobshavn Isbræ, Greenland. *Journal of Geophysical Research*, *115*, F01005. <https://doi.org/10.1029/2009JF001405>
- Arp, C. D., Jones, B. M., Whitman, M., Larsen, A., & Urban, F. E. (2010). Lake temperature and ice cover regimes in the Alaskan subarctic and Arctic: Integrated monitoring, remote sensing, and modeling. *Journal of the American Water Resources Association*, *46*(4), 777–791. <https://doi.org/10.1111/j.1752-1688.2010.00451.x>
- Åström, J. A., Riikilä, T. I., Tallinen, T., Zwinger, T., Benn, D., Moore, J. C., & Timonen, J. (2013). A particle based simulation model for glacier dynamics. *The Cryosphere*, *7*(5), 1591–1602. <https://doi.org/10.5194/tc-7-1591-2013>
- Benn, D. I., Åström, J. A. N., Zwinger, T., Todd, J. O. E., Nick, F. M., Cook, S., et al. (2017). Melt-under-cutting and buoyancy-driven calving from tidewater glaciers: New insights from discrete element and continuum model simulations. *Journal of Glaciology*, *63*(240), 691–702. <https://doi.org/10.1017/jog.2017.41>
- Benn, D. I., Warren, C. R., & Mottram, R. H. (2007). Calving processes and the dynamics of calving glaciers. *Earth-Science Reviews*, *82*(3–4), 143–179. <https://doi.org/10.1016/j.earscirev.2007.02.002>
- Boyce, E. S., Motyka, R. J., & Truffer, M. (2007). Flotation and retreat of a lake-calving terminus, Mendenhall Glacier, Southeast Alaska, USA. *Journal of Glaciology*, *53*(181), 211–224. <https://doi.org/10.3189/172756507782202928>
- Carrivick, J. L., & Quincey, D. J. (2014). Progressive increase in number and volume of ice-marginal lakes on the western margin of the Greenland ice sheet. *Global and Planetary Change*, *116*, 156–163. <https://doi.org/10.1016/j.gloplacha.2014.02.009>
- Carrivick, J. L., & Tweed, F. S. (2013). Proglacial lakes: Character, behaviour and geological importance. *Quaternary Science Reviews*, *78*, 34–52. <https://doi.org/10.1016/j.quascirev.2013.07.028>
- Carrivick, J. L., & Tweed, F. S. (2019). A review of glacier outburst floods in Iceland and Greenland with a megafloods perspective. *Earth-Science Reviews*, *196*, 102876. <https://doi.org/10.1016/j.earscirev.2019.102876>
- Carrivick, J. L., Tweed, F. S., Ng, F., Quincey, D. J., Mallalieu, J., Ingeman-Nielsen, T., et al. (2017). Ice-dammed lake drainage evolution at Russell Glacier, West Greenland. *Frontiers in Earth Science*, *5*, 100. <https://doi.org/10.3389/feart.2017.00100>
- Cassotto, R., Fahnestock, M., Amundson, J. M., Truffer, M., & Joughin, I. (2015). Seasonal and interannual variations in ice mélange and its impact on terminus stability, Jakobshavn Isbræ, Greenland. *Journal of Glaciology*, *61*(225), 76–88. <https://doi.org/10.3189/2015JG13J235>
- Chapuis, A., & Tetzlaff, T. (2014). The variability of tidewater-glacier calving: Origin of event-size and interval distributions. *Journal of Glaciology*, *60*(222), 622–634. <https://doi.org/10.3189/2014JG13J215>
- Christoffersen, P., Muggford, R. I., Heywood, K. J., Joughin, I., Dowdeswell, J. A., Syvitski, J. P. M., et al. (2011). Warming of waters in an East Greenland fjord prior to glacier retreat: Mechanisms and connection to large-scale atmospheric conditions. *The Cryosphere*, *5*(3), 701–714. <https://doi.org/10.5194/tc-5-701-2011>
- Demidov, I. N., Houmark-Nielsen, M., Kjaer, K. H., & Larsen, E. (2006). The last Scandinavian ice sheet in northwestern Russia: Ice flow patterns and decay dynamics. *Boreas*, *35*(3), 425–443. <https://doi.org/10.1080/03009480600781883>
- Diolaiuti, G., Citterio, M., Carnielli, T., D'agata, C., Kirkbride, M., & Smiraglia, C. (2006). Rates, processes and morphology of freshwater calving at Miage Glacier (Italian Alps). *Hydrological Processes*, *20*(10), 2233–2244. <https://doi.org/10.1002/hyp.6198>
- Duguay, C. R., Prowse, T. D., Bonsal, B. R., Brown, R. D., Lacroix, M. P., & Menard, P. (2006). Recent trends in Canadian lake ice cover. *Hydrological Processes*, *20*(4), 781–801. <https://doi.org/10.1002/hyp.6131>
- Dykes, R. C., Brook, M. S., Robertson, C. M., & Fuller, I. C. (2011). Twenty-first century calving retreat of Tasman Glacier, Southern Alps, New Zealand. *Arctic Antarctic and Alpine Research*, *43*(1), 1–10. <https://doi.org/10.1657/1938-4246-43.1.1>
- Eltner, A., Kaiser, A., Castillo, C., Rock, G., Neugirg, F., & Abellán, A. (2016). Image-based surface reconstruction in geomorphometry—Merits, limits and developments. *Earth Surface Dynamics*, *4*(2), 359–389. <https://doi.org/10.5194/esurf-4-359-2016>
- Gillet-Chaulet, F., Gagliardini, O., Seddik, H., Nodet, M., Durand, G., Ritz, C., et al. (2012). Greenland ice sheet contribution to sea-level rise from a new-generation ice-sheet model. *The Cryosphere*, *6*(6), 1561–1576. <https://doi.org/10.5194/tc-6-1561-2012>
- Hanna, E., Navarro, F. J., Pattyn, F., Domingues, C. M., Fettweis, X., Ivins, E. R., et al. (2013). Ice-sheet mass balance and climate change. *Nature*, *498*(7452), 51–59. <https://doi.org/10.1038/nature12238>
- Haresign, E., & Warren, C. R. (2005). *Melt rates at calving termini: A study at Glacier León, Chilean Patagonia, Special Publications*, (Vol. 242, pp. 99–109). London: Geological Society.
- How, P., Schild, K. M., Benn, D. I., Noormets, R., Kirchner, N., Luckman, A., et al. (2019). Calving controlled by melt-under-cutting: Detailed calving styles revealed through time-lapse observations. *Annals of Glaciology*, *60*(78), 20–31. <https://doi.org/10.1017/aog.2018.28>
- Howat, I. M., Box, J. E., Ahn, Y., Herrington, A., & McFadden, E. M. (2010). Seasonal variability in the dynamics of marine-terminating outlet glaciers in Greenland. *Journal of Glaciology*, *56*(198), 601–613. <https://doi.org/10.3189/002214310793146232>
- Jiang, Y., Dixon, T. H., & Wdowinski, S. (2010). Accelerating uplift in the North Atlantic region as an indicator of ice loss. *Nature Geoscience*, *3*(6), 404–407. <https://doi.org/10.1038/ngeo845>
- Joughin, I., Howat, I. M., Fahnestock, M., Smith, B., Krabill, W., Alley, R. B., et al. (2008). Continued evolution of Jakobshavn Isbræ following its rapid speedup. *Journal of Geophysical Research*, *113*, F04006. <https://doi.org/10.1029/2008JF001023>
- Joughin, I., Smith, B. E., Howat, I. M., Scambos, T., & Moon, T. (2010). Greenland flow variability from ice-sheet-wide velocity mapping. *Journal of Glaciology*, *56*(197), 415–430. <https://doi.org/10.3189/002214310792447734>
- Khan, S. A., Aschwanden, A., Björk, A. A., Wahr, J., Kjeldsen, K. K., & Kjaer, K. H. (2015). Greenland ice sheet mass balance: A review. *Reports on Progress in Physics*, *78*, 046801. <https://doi.org/10.1088/0034-4885/78/4/046801>
- King, O., Dehecq, A., Quincey, D., & Carrivick, J. (2018). Contrasting geometric and dynamic evolution of lake and land-terminating glaciers in the central Himalaya. *Global and Planetary Change*, *167*, 46–60. <https://doi.org/10.1016/j.gloplacha.2018.05.006>
- Kirkbride, M. P. (1993). The temporal significance of transitions from melting to calving termini at glaciers in the central Southern Alps of New Zealand. *The Holocene*, *3*(3), 232–240. <https://doi.org/10.1177/095968369300300305>
- Kjeldsen, K. K., Korsgaard, N. J., Björk, A. A., Khan, S. A., Box, J. E., Funder, S., et al. (2015). Spatial and temporal distribution of mass loss from the Greenland ice sheet since AD 1900. *Nature*, *528*(7582), 396–400. <https://doi.org/10.1038/nature16183>
- Mallalieu, J., Carrivick, J. L., Quincey, D. J., Smith, M. W., & James, W. H. M. (2017). An integrated structure-from-motion and time-lapse technique for quantifying ice-margin dynamics. *Journal of Glaciology*, *63*(242), 937–949. <https://doi.org/10.1017/jog.2017.48>
- Medrzycka, D., Benn, D. I., Box, J. E., Copland, L., & Balog, J. (2016). Calving behavior at Rink Isbræ, West Greenland, from time-lapse photos. *Arctic Antarctic and Alpine Research*, *48*(2), 263–277. <https://doi.org/10.1657/AAAR0015-059>

- Minowa, M., Podolskiy, E. A., Sugiyama, S., Sakakibara, D., & Skvarca, P. (2018). Glacier calving observed with time-lapse imagery and tsunami waves at Glaciar Perito Moreno, Patagonia. *Journal of Glaciology*, *64*(245), 362–376. <https://doi.org/10.1017/jog.2018.28>
- Murray, T., Selmes, N., James, T. D., Edwards, S., Martin, I., O'farrell, T., et al. (2015). Dynamics of glacier calving at the ungrounded margin of Helheim Glacier, southeast Greenland. *Journal of Geophysical Research: Earth Surface*, *120*, 964–982. <https://doi.org/10.1002/2015JF003531>
- Nick, F. M., Vieli, A., Andersen, M. L., Joughin, I., Payne, A., Edwards, T. L., et al. (2013). Future sea-level rise from Greenland's main outlet glaciers in a warming climate. *Nature*, *497*(7448), 235–238. <https://doi.org/10.1038/nature12068>
- Perkins, A. J., & Brennand, T. A. (2015). Refining the pattern and style of Cordilleran ice sheet retreat: Palaeogeography, evolution and implications of lateglacial ice-dammed lake systems on the southern Fraser Plateau, British Columbia, Canada. *Boreas*, *44*(2), 319–342. <https://doi.org/10.1111/bor.12100>
- Purdie, H., Bealing, P., Tidey, E., Gomez, C., & Harrison, J. (2016). Bathymetric evolution of Tasman Glacier terminal lake, New Zealand, as determined by remote surveying techniques. *Global and Planetary Change*, *147*, 1–11. <https://doi.org/10.1016/j.gloplacha.2016.10.010>
- Rignot, E., Fenty, I., Xu, Y., Cai, C., & Kemp, C. (2015). Undercutting of marine-terminating glaciers in West Greenland. *Geophysical Research Letters*, *42*, 5909–5917. <https://doi.org/10.1002/2015GL064236>
- Rignot, E., & Mouginot, J. (2012). Ice flow in Greenland for the international polar year 2008–2009. *Geophysical Research Letters*, *39*, L11501. <https://doi.org/10.1029/2012GL051634>
- Röhl, K. (2006). Thermo-erosional notch development at fresh-water-calving Tasman Glacier, New Zealand. *Journal of Glaciology*, *52*(177), 203–213. <https://doi.org/10.3189/172756506781828773>
- Russell, A. J., Carrivick, J. L., Ingeman-Nielsen, T., Yde, J. C., & Williams, M. (2011). A new cycle of jokulhlaups at Russell Glacier, Kangerlussuaq, West Greenland. *Journal of Glaciology*, *57*(202), 238–246. <https://doi.org/10.3189/002214311796405997>
- Ryan, J. C., Hubbard, A. L., Box, J. E., Todd, J., Christoffersen, P., Carr, J. R., et al. (2015). UAV photogrammetry and structure from motion to assess calving dynamics at Store Glacier, a large outlet draining the Greenland ice sheet. *The Cryosphere*, *9*(1), 1–11. <https://doi.org/10.5194/tc-9-1-2015>
- Smejkalova, T., Edwards, M. E., & Dash, J. (2016). Arctic lakes show strong decadal trend in earlier spring ice-out. *Scientific Reports*, *6*, 38449. <https://doi.org/10.1038/srep38449>
- Stokes, C. R., & Clark, C. D. (2003). The Dubawnt Lake palaeo-ice stream: Evidence for dynamic ice sheet behaviour on the Canadian Shield and insights regarding the controls on ice-stream location and vigour. *Boreas*, *32*(1), 263–279. <https://doi.org/10.1111/j.1502-3885.2003.tb01442.x>
- Stokes, C. R., & Clark, C. D. (2004). Evolution of late glacial ice-marginal lakes on the northwestern Canadian Shield and their influence on the location of the Dubawnt Lake palaeo-ice stream. *Palaeogeography Palaeoclimatology Palaeoecology*, *215*(1–2), 155–171. [https://doi.org/10.1016/S0031-0182\(04\)00467-5](https://doi.org/10.1016/S0031-0182(04)00467-5)
- Surdu, C. M., Duguay, C. R., & Prieto, D. F. (2016). Evidence of recent changes in the ice regime of lakes in the Canadian High Arctic from spaceborne satellite observations. *The Cryosphere*, *10*(3), 941–960. <https://doi.org/10.5194/tc-10-941-2016>
- Truffer, M., & Motyka, R. J. (2016). Where glaciers meet water: Subaqueous melt and its relevance to glaciers in various settings. *Reviews of Geophysics*, *54*(1), 220–239. <https://doi.org/10.1002/2015RG000494>
- Trussel, B. L., Motyka, R. J., Truffer, M., & Larsen, C. F. (2013). Rapid thinning of Lake-Calving Yakutat Glacier and the collapse of the Yakutat Icefield, Southeast Alaska, USA. *Journal of Glaciology*, *59*(213), 149–161. <https://doi.org/10.3189/2013JOG12J081>
- Tsutaki, S., Nishimura, D., Yoshizawa, T., & Sugiyama, S. (2011). Changes in glacier dynamics under the influence of proglacial lake formation in Rhonegletscher, Switzerland. *Annals of Glaciology*, *52*(58), 31–36. <https://doi.org/10.3189/172756411797252194>
- Tsutaki, S., Sugiyama, S., Nishimura, D., & Funk, M. (2013). Acceleration and flotation of a glacier terminus during formation of a proglacial lake in Rhonegletscher, Switzerland. *Journal of Glaciology*, *59*(215), 559–570. <https://doi.org/10.3189/2013JOG12J107>
- Van Den Broeke, M., Bamber, J., Ettema, J., Rignot, E., Schrama, E., Van De Berg, W. J., et al. (2009). Partitioning recent Greenland mass loss. *Science*, *326*(5955), 984–986. <https://doi.org/10.1126/science.1178176>
- Van Den Broeke, M. R., Enderlin, E. M., Howat, I. M., Kuipers, M. P., Noël, B. P. Y., Van De Berg, W. J., et al. (2016). On the recent contribution of the Greenland ice sheet to sea level change. *The Cryosphere*, *10*(5), 1933–1946. <https://doi.org/10.5194/tc-10-1933-2016>
- Velicogna, I. (2009). Increasing rates of ice mass loss from the Greenland and Antarctic ice sheets revealed by GRACE. *Geophysical Research Letters*, *36*, L19503. <https://doi.org/10.1029/2009GL040222>
- Vieli, A., Jania, J., & Kolondra, L. (2002). The retreat of a tidewater glacier: Observations and model calculations on Hansbreen, Spitsbergen. *Journal of Glaciology*, *48*(163), 592–600. <https://doi.org/10.3189/172756502781831089>
- Warren, C. R., Greene, D. R., & Glasser, N. F. (1995). Glacier Upsala, Patagonia: Rapid calving retreat in fresh water. *Annals of Glaciology*, *21*, 311–316. <https://doi.org/10.3189/S0260305500015998>
- Xie, S., Dixon, T. H., Holland, D. M., Voytenko, D., & Vaňková, I. (2019). Rapid iceberg calving following removal of tightly packed pro-glacial mélange. *Nature Communications*, *10*(1), 3250–3215. <https://doi.org/10.1038/s41467-019-10908-4>